Int. J. Impact Engng Vol. 9, No. 4, pp. 455–474, 1990
Printed in Great Britain

0734–743X/90 $3.00 + 0.00
Pergamon Press plc

A SIMPLE ONE-DIMENSIONAL APPROACH TO MODELLING CERAMIC COMPOSITE ARMOUR DEFEAT

RAYMOND L. WOODWARD
Department of Defence, Materials Research Laboratory, Defence Science and Technology Organisation, P.O. Box 50, Ascot Vale, Victoria 3032, Australia

(*Received* 30 *March* 1990; *and in revised form* 22 *June* 1990)

Summary—This work develops a simple set of models for the perforation of ceramic composite armour, which highlight the essential physical processes and illustrate approximately the dependency of ballistic resistance on physical properties and impact parameters. The major features of ceramic composite armour failure (viz. fracture conoid formation, dishing failure of thin backing plates, perforation of thick packing plates, and projectile erosion) are combined with a lumping of masses to treat material acceleration to produce simple models which allow computations on ceramic targets with both thin and thick metallic backings. Calculations are compared with a broad range of empirical data and are also used to discuss aspects of the interaction of penetrators with ceramic composite armours. The good correlation of models with experiment demonstrates the usefulness of the present approach for studying ceramic composite armour defeat.

NOTATION

A, B	material constants
A_0	penetrator area of cross section
b	backing thickness
c	ceramic thickness
D_0, D_R, D_P	diameter of base of cone, base of cone after erosion, and penetrator, respectively
E_k	Kinetic energy of projectile, ceramic and backing after target acceleration
F	force
h	displacement of backing
M	mass
n	material constant (work hardening exponent)
t	time
$U, \dot{U}, \ddot{U}$	displacement, velocity and acceleration, respectively
W	work
Y	yield stress, flow stress or erosion pressure
P, I, C, T	subscripts: penetrator, interface, ceramic and target, respectively
Δ	small increase
ρ	density
π	number (3.14159 . . .)
Σ	summation operator
σ	effective stress
$\varepsilon, \bar{\varepsilon}, \varepsilon_i$	strain, effective strain, instability strain
θ	bend angle of dishing

1. INTRODUCTION

The development of ceramic composite armours rests soundly on the basis of the work of Wilkins *et al.* [1–3] who developed the commonly used configuration of ceramic tiles supported by a thin ductile backing material. Wilkins used the HEMP finite difference computer code to simulate ballistic experiments, and although a complete description of an event through to perforation was not possible, he was able to isolate many of the important features of the penetration problem. The ceramic tile was seen to load the projectile nose causing attrition and deceleration, at a rate governed by the yield strength of the projectile material. The ceramic fractured in the form of a conoid followed by tensile failure in the ceramic initiating at the ceramic/backing plate interface, opposite the impact location. Wilkins proposed that delaying the initiation of tensile failure would substantially increase the performance of ceramic composite armours by allowing more projectile erosion.

There has been substantial interest recently in empirical studies of the failure of ceramic armour. Mayseless *et al.* [4] present data for targets with a range of thin backing plate materials, and also for cases where no backing is used. The backing is shown to contribute substantially to the achievement of good ballistic performance in the ceramic. Rosenberg *et al.* [5,6] have used effectively semi-infinite backings and measured residual penetration depths into these as a guide to ceramic performance. They conclude that ballistic performance increases with increase in effective compressive strength of the ceramic. A similar technique has been used by Mellgard *et al.* [7].

Studies [8,9] of the energy distribution in the defeat of glass and ceramic tiles backed by thin aluminium plates, using small calibre armour piercing projectiles, demonstrated that a negligible proportion of the projectile's kinetic energy ($\sim 0.2\%$) went into fracture of the ceramic. The major energy dissipating mechanisms were identified as plastic deformation of both the backing plate (20–40%) and the penetrator (10–15%), and kinetic energy picked up by the ceramic debris (45–70%). The backing plates for ceramic targets were not defeated by perforation, but rather bulged and necked to failure by ductile fracture. In the case of glass tiles the projectile core was not deformed by the glass and defeated the backing plate by perforation. These results suggest that a major aspect of the interaction is the transfer of momentum from the impacting projectile to a larger volume of ceramic which is ejected at high velocity. High speed cine and flash radiography confirm that momentum is conserved by the impulse delivered to the target producing a small forward velocity of the centre of mass of the impacted target. The high ejection velocity of fragmented glass debris, similar to the rate of projectile penetration, in the photographs of impacted glass by Pavel *et al.* [10] confirms the important part played by the transfer of momentum.

While cone cracking has been studied extensively [11–15] in semi-infinite glass media, it has been studied less extensively in finite thickness bodies [16]. The ideal cone angle depends on the elastic properties of both indenter and brittle material [12], but for quasi-static ball identations is generally around 68° to the axis of indentation. Under controlled dynamic conditions the crack travels through a time varying stress field and hence significant, but predictable, departures from the ideal angle are observed [12]. Ballistic impact tends to be an overload situation with little control and therefore it is extremely difficult to study the sequence of cracking. Nevertheless the cone shaped zone of damage simulated by Wilkins [3] is similar to observed fracture conoids and at similar angles to cone cracks seen in quasi-static indentation of glass plates. Hornemann *et al.* [17] have used high speed photography to study crack propagation in the ballistic impact of glass plates. They observe not only the propagation of cracks from the impact site but also the nucleation and growth of cracks in the stress field ahead of the damage front.

Studies of impact and shock loaded ceramics [18–20] show that the Hugoniot elastic limit does not correlate in a simple manner with indications of microplastic yielding, and the fracture behaviour of ceramics is not simply interpreted in terms of the stress state. There is no clear correlation between the degree of ceramic fragmentation and ballistic resistance [21,22], with extremely tough ceramics such as the toughened zirconias showing no better ballistic performance than alumina ceramics. This is as would be expected given that less than 1% of the projectile impact kinetic energy appears as fracture energy [8,9]. The degree of break-up in ballistic tests does however correlate well with ceramic toughness [8,9,21]. Tests on ceramics with a thick backing have shown that ballistic resistance is related to strength, although the appropriate strength parameter does not appear to be simply the Hugoniot elastic limit or the ceramic compressive strength [5,6]. It is noted that ceramic powders confined by a hydrostatic pressure can exhibit a significant effective flow stress [23], and confined ceramic powders themselves can provide substantial resistance to ballistic impact [24].

The experimental and computational studies leave many gaps in our understanding of the perforation of ceramics. This work presents approximate model solutions which allow computations on ballistic impacts into ceramic composite armours, with both thick backing and thin backing, relative to the projectile calibre. The cone crack formation, ceramic and projectile erosion and backing deformation as well as the inertial response of the system

components are realistically modelled. The principle observed features associated with trends in ballistic performance with changes in ceramic and backing thickness, ceramic and backing materials, projectile type and impact velocity are observed in the computational results. Predictions are generally of the correct magnitude and in many cases quite accurate. The solutions allow the mechanical principles to be studied, and can direct attention to those aspects, such as ceramic strength properties relevant to cracking and erosion, which need to be more closely studied.

2. MODEL DEVELOPMENT

(*a*) *Approximate numerical considerations*

From the examination of computer simulations and corresponding impact experiments Wilkins [2] concluded that the force retarding a projectile, which has impacted a ceramic, is governed by plastic yielding of the projectile. The force acting on the ceramic then, can be estimated as the yield force of the projectile plus the rate of change in momentum according to Tate's [25] approximate theory of penetration. Taking a typical simulation sequence from the work of Wilkins [3], it is a simple matter to show that the acceleration of the mass of ceramic bounded by the cone crack as well as the mass of the contiguous section of backing plate which is dishing, is consistent with a velocity field profile with conical symmetry in that region and the resultant force acting on the target. The resultant force acting on a target is calculated as the difference between that acting on the ceramic due to the projectile, as above, and the resisting force provided by the backing due to simple dishing deformation as estimated by plasticity calculations. It is therefore possible to state with a high degree of certainty that resistance to penetrator motion is provided by inertia of the ceramic and the backing bounded by the cone crack, and by dishing deformation of the backing. Using such simple calculations it is also possible to show that at the time when the projectile has decelerated and target material accelerated to a common intermediate velocity, the displacement of the back of the target is only a few millimetres, in contrast to final deflections of 15–25 mm observed in typical perforated aluminium backing plates. The conclusion therefore is that a second stage of perforation involves the penetrator and target material bounded by the cone, moving forward resisted by bending and membrane forces in the backing, till either they are slowed to zero velocity or rupture of the backing occurs. These concepts form the basis for modelling the perforation of ceramic composites with thin backing plates.

(*b*) *Physical concepts and assumptions*

The main features associated with perforation of a ceramic armour with a thin backing plate are shown schematically in Fig. 1(a). In modelling the process, it was assumed that crack propagation was sufficiently fast compared with the projectile velocity that the cone crack separates the loaded region inside the cone from an unloaded region outside the cone. Based on the approximate calculations outlined previously, the ceramic inside the cone and the backing plate bounded by the base of the cone are accelerated forward with a velocity profile allowing compatibility with both the flat ended projectile and the dishing of the backing plate. As shown in Fig. 1(b) this more realistic velocity profile was slightly modified for computational efficacy in the model, the effect of this change being negligible as the base diameter of the cone is generally far greater than the projectile diameter. Because of the lack of knowledge on cone angle as a function of impact parameters, it was decided to use an angle between the normal to the ceramic surface and the cone side of 68° for all computations, at least consistent with quasi-static observations on simple systems.

At the front of the penetrator erosion of projectile material is taking place, the term erosion implying a physical separation of material so that its momentum no longer contributes to target perforation. In practice with brittle penetrator materials this may be in "chunks", however as the physics of such an attrition process is not developed it was assumed that projectile erosion, whether by a cracking or a shearing mechanism, was governed by plastic flow of the penetrator material. Similarly if the velocity is high enough,

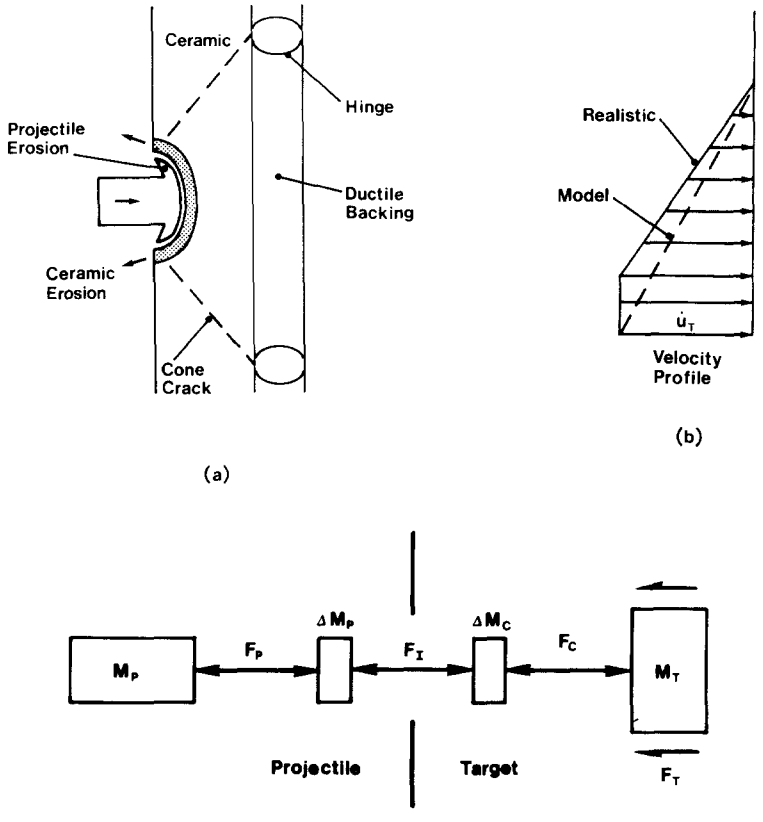

FIG. 1. Basic concepts of the interaction of a penetrator with a ceramic tile backed by a thin ductile plate. (a) Schematic of the eroding penetrator, eroding ceramic material, cone crack and positions of the hinges for dishing of the backing. (b) Assumed velocity distribution in the ceramic and backing during the first stage of acceleration. The more realistic distribution has a constant velocity from the axis to the projectile diameter, however a slightly modified distribution was used in the model for computational simplicity. (c) Lumped mass model, where the masses M and connecting forces F are defined in the text. In a small time step masses ΔM_p and ΔM_c are eroded from the projectile and ceramic, respectively.

yielding and fracture of the front of the ceramic will be observed. This is again considered as leading to erosion of ceramic in contact with the projectile, governed by the normal load which the ceramic can sustain. The measure and physical interpretation of the load at which ceramic erosion occurs is discussed in relation to the comparison of model computations to experimental data, below.

The lumped parameter model for the inertial response of the system is represented schematically in Fig. 1(c). In any time step Δt a mass ΔM_p and a mass ΔM_c of projectile and ceramic, respectively, are eroded. M_p is the oncoming projectile mass and M_T the mass of target material, ceramic bounded by the cone crack and contiguous backing material, being accelerated. Force F_p resists forward movement of the projectile and F_T resists acceleration of the target material. F_C is a measure of the strength or collapse load of the ceramic and at the interface F_I is determined by ceramic and penetrator strengths and the rate of ceramic and penetrator erosion. After some time of interaction a number of consequences can ensue, viz. the system can slow to zero velocity stopping the projectile, or the projectile can be completely eroded and thus stopped. The ceramic can be eroded to zero thickness and if there is still a velocity difference between the projectile and the backing, the projectile may perforate or, if there is no residual velocity difference, the backing may continue to bulge till either the velocity is reduced to zero or bursting of the bulge occurs. Without complete ceramic erosion the components may come to some

constant intermediate velocity and perforation occur if the residual momentum is sufficient to continue bulging of the backing plate and cause rupture. The model for ceramic composite armours with thin backing is divided into two stages which treat target acceleration using the model of Fig. 1(c), followed by an examination of target failure.

(*c*) *Target acceleration*

The equations of motion of the system in Fig. 1(c) are;

$$F_P = -M_P\dot{U}_P, \tag{1a}$$

$$F_I - F_P = -\Delta M_P\dot{U}_P/\Delta t, \tag{1b}$$

$$F_C - F_I = -\Delta M_C\dot{U}_C/\Delta t, \tag{1c}$$

$$F_T - F_C = -M_T\dot{U}_T, \tag{1d}$$

where F is force, M is mass, Δt is the time increment, $\dot{U}$ and $\ddot{U}$ are velocity and acceleration, respectively (both positive in the direction of initial projectile motion), and subscripts P, I, C and T refer to penetrator, interface, ceramic and target, respectively, as in Fig. 1(c).

Each of Eqns (1) relates the force on an element to the change in momentum by either acceleration $\ddot{U}$, or mass change ΔM. The sign in Eqn (1b) is such that if $F_I > F_P$, ΔM_P is negative, i.e. there is a mass loss from the penetrator. The sign in Eqn (1c) is such that if $F_I > F_C$, $\Delta M_C\dot{U}_C$ is positive, i.e. there is an increase in momentum of the ceramic material which is moved out of the way. At the interface the approach of the penetrator and target in time step Δt is related to the loss in mass of penetrator and target. As a flat ended cylindrical penetrator of cross sectional area A_0 is being treated, we can imagine a column of penetrator and ceramic being squeezed out giving continuity equations of the form;

$$\Delta M_P/\rho_P A_0 = -(\dot{U}_P - \dot{U}_C)\Delta t, \tag{2a}$$

$$\Delta M_C/\rho_C A_0 = -(\dot{U}_C - \dot{U}_T)\Delta t, \tag{2b}$$

where ρ is the material density.

Constitutive equations for the failure of penetrator and ceramic can be established by requiring that for erosion of a column of material to occur, a value of flow stress Y, must be exceeded, whether this is governed by uniaxial yield stress, hardness or some other measure of strength. Then for erosion to occur

$$F_P = Y_P A_0, \tag{3a}$$

$$F_C = Y_C A_0, \tag{3b}$$

In the course of solving the equations, erosion of both ceramic and penetrator did not necessarily occur; erosion requires that F_I in Eqn (1) exceed the relevant force F_P or F_C.

Equations (1)–(3) represent a very simplified concept of the interaction, with gross assumptions on the lumping of elements of material into composite masses. The view of ceramic compression in a simple column is expedient and the issue of failure or erosion stress level for the ceramic must be addressed. The contribution of radial inertia to projectile deceleration is ignored, as it is difficult to include in the form developed by Johnson [26], as erosion in a single front element leads to the force becoming unrealistically large as the time step, and hence the height of that front eroding element also, becomes small. Elimination of $\dot{U}_C$ and ΔM_C from the equations yields a quadratic which can be solved at each time step for the only unknown parameter, the penetrator mass loss ΔM_P. At each time step all other parameters can be updated and the solution then repeated. A relationship is required for the resistance of the target backing to bulging F_T and for an appropriate mass distribution to give the effective mass M_T.

Woodward *et al.* [9] derive an equation for the work W, to dish a plate of thickness b and flow stress Y_T to a displacement h,

$$W = \pi bhY_T(2/3b + 1/2h) \tag{4}$$

and it is shown that this equation gives reasonable estimates of the work done on dished

backings from actual impacted ceramic composite targets, when compared with the work calculated from measurements on the plate profile. In deriving Eqn (4) it was assumed the dish was in the form of a cone for calculation of stretching work, a yield moment was assumed for bending, and it was noted that the work done in tangential curvature in the conically dished region equals the work done in radial curvature (Johnson [27]). The force resisting dishing is thus obtained by differentiating Eqn (4) to give

$$F_T = \pi b Y_T(2/3b + h). \tag{5}$$

If M_C and M_B represent masses of elements of ceramic and backing travelling at velocities $\dot{U}_C$ and $\dot{U}_B$, respectively, then the total momentum is obtained by summing the momenta of individual elements. If the velocity of target material beneath the penetrator is $\dot{U}_T$, then the effective mass of the target material in Fig. 1(c), M_T, can be defined by

$$M_T\dot{U}_T = \Sigma M_C\dot{U}_C + \Sigma M_B\dot{U}_B. \tag{6}$$

For the modified velocity distribution represented in Fig. 1(b) combined with the mass distribution of the ceramic cone and backing in Fig. 1(a), the effective mass becomes approximately

$$M_T = \pi D_0(\rho_C c/2 + \rho_B b)/12, \tag{7}$$

where D_0 is the base diameter of the cone, c is the ceramic tile thickness, and other symbols and subscript notation are as used before. In cases where ceramic erosion occurred, the mass distribution was allowed to shrink in a geometrically similar manner, with the velocity dropping to zero at the new outer boundary of cone intersection with the backing. Thus D_0 in Eqn (7) simply reduces to a new diameter proportional to the new height of the conical section. This approximation takes some account of the reduced target mass being accelerated and the reduced area of backing material which is subjected to bending and stretching loads.

(d) Target failure

Two target failure possibilities are considered in order. For the first involving ductile instability in the backing plate, the situation after the phase of accelerating the target material is depicted in Fig. 2(a) with ceramic still separating the projectile from the backing plate and with projectile and backing moving forward at the same velocity. In this situation bulging of the backing plate will continue with the kinetic energy of the system being dissipated in plastic deformation of the backing, terminated by either a reduction to zero velocity or rupture as in Fig. 2(b). In practice the hinge in the backing plate may be expected to move radially and substantial elastic deflections occur, particularly in thin plates. These aspects are, however, not easily treated. The simplified approach used to obtain a solution considers the bulging plate as ideally plastic, with the hinge located at the cone base and uses Eqn (4) to calculate the work done. Perforation occurs if there is sufficient kinetic energy left in the projectile, ceramic and backing after the acceleration phase to continue plate bulging to rupture. Thus a bulge height at plate rupture is required, i.e. a failure criterion.

Backing material stress/strain properties were curve fit to an equation of the form

$$\sigma = A + B\varepsilon^n, \tag{8}$$

where σ and ε are effective stress and strain, and A, B and n are constant curve fitting parameters for the material. The strain at instability ε_i in a biaxial tension test can then be obtained by solving the equation

$$11B\varepsilon_i^{n+1} - 4(2n+1)B\varepsilon_i^n + 11A\varepsilon_i - 4A = 0, \tag{9}$$

which is a variation on the form used by Johnson and Mellor [28] because of the different curve fitting relationship for stress and strain, Eqn (8). Equation (9) is easily solved iteratively by computer. For hydraulic bulging of circular plates the strain at instability can be related to the displacement using the assumption that the particles in the membrane

describe circular paths. For the velocity profile of Fig. 2(b), the backing plate is going to deform into the shape of a cone. For simplicity it was assumed that the cone is uniformly tapered from the instability strain at the centre ε_i to the thickness of the original plate at the cone diameter D_0. Then if θ is the angle between the base and side of the cone, as in Fig. 2(b), constant volume deformation requires

$$\varepsilon_i = \ln(3 \cos \theta - 2). \tag{10}$$

Thus from the material characteristics, Eqn (8), the instability strain is calculated using Eqn (9), which is substituted into Eqn (10) to obtain the angle through which the sides of the cone are bent at failure. From simple geometry the displacement h of the cone is calculated and this is substituted into Eqn (4) to calculate the dishing work.

If ceramic erosion has occurred during the target acceleration phase then the area of the backing that is loaded will be reduced as discussed earlier. The assumed reduced dimensions of the cone and loaded backing after the target acceleration stage are shown schematically in Fig. 2(c), in relation to the initial dimensions. The velocity profile is shown in Fig. 2(d), where it is assumed for computational ease that the velocity drops to zero at the reduced outer hinge diameter D_R. The reduced diameter combined with the deflection angle at failure from Eqn (10) leads to a lower failure displacement and hence work done in dishing failure using Eqn (4), than would be the case if no ceramic erosion occurred. It

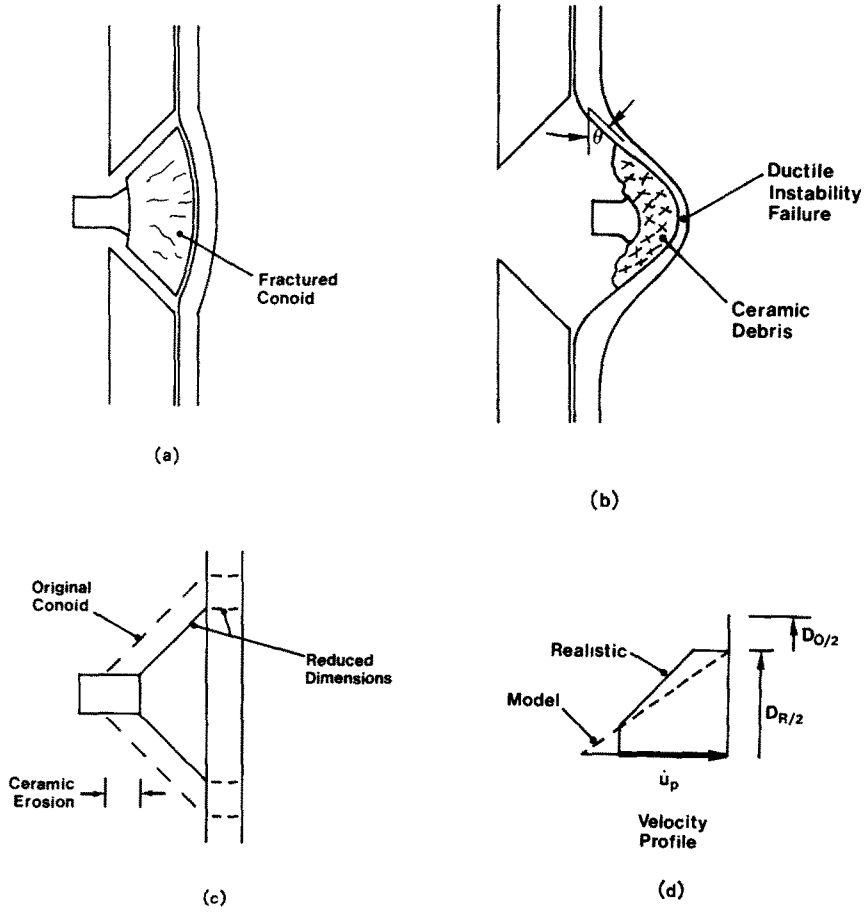

FIG. 2. Second stage of perforation of the ceramic tile with a thin backing where (a) the projectile, ceramic and backing move as a unit until (b) a biaxial tensile failure of the sheet occurs at an angle of bend θ. (c) The assumed reduction in effective dimensions of the loaded conoid and backing plate as a result of ceramic erosion. (d) Velocity distribution in the second stage where the more realistic distribution has a step near the reduced conoid outer diameter, but a simpler form is assumed for ease of computation.

was assumed that only the momentum of the projectile, the ceramic and the backing material within the reduced dimensions acted to continue bulging. Thus using the simpler velocity distribution of Fig. 2(d) the effective kinetic energy E_K to equate to the work done by Eqn (4) is

$$E_K = 1/2M_P\dot{U}_P^2 + \pi/8(\rho_C c/5 + \rho_B b/3)D_R^4 U_T^2/(D_R - D_P)^2 \tag{11}$$

where the ceramic thickness c is the reduced thickness after erosion, and D_P is the penetrator diameter. The effects of using reduced dimensions when accounting for the effects of erosion will be discussed in considering sample computations.

If the ceramic is eroded to zero thickness during target acceleration, then a projectile of higher relative velocity bears on the backing material and an alternative second failure criterion is needed. For failure under these circumstances it was considered the velocity at which the backing was moving did not contribute to perforation and that it was the difference in projectile/target velocity which allowed perforation. Thus the equation to determine whether the penetrator would perforate in this case was

$$1/2M_P(\dot{U}_B - \dot{U}_P)^2 = \pi D_P^2 b Y_T/2, \tag{12}$$

where Y_T is the target flow stress, and subscript B represents backing. The method assumes a simple ductile hole formation mode of failure and the equation is due to Taylor [29,30].

The set of equations described for the acceleration and failure stages were written into a computer program which treats perforation of ceramic composite targets with thin backing plates. Examples of computations performed with the method are compared with experimental data below.

(e) Composites with thick backing

For cases with very thick backing materials it was found that the ceramic can be completely eroded with a relatively small increase in velocity of the backing. In addition the treatment of thick plate perforation with a dishing model is inappropriate. Therefore a simplified model for the first phase was developed where the interaction of the penetrator and the ceramic only are considered, with the thick backing remaining stationary. The residual penetrator, after eroding the ceramic, then interacts with the backing using a plugging model for finite thicknesses or a deep penetration model for effectively semi-infinite backings. The method also has the advantage of allowing direct checking of the ceramic erosion model against data of the type produced by Rosenberg *et al.* [5,6] using semi-finite targets.

The concept of interaction with a thick target is shown in Fig. 3(a) and the lumped parameter model is illustrated in Fig. 3(b). It is assumed that spreading of the load by the ceramic conoid is sufficient to allow negligible yielding of the backing plate. Then for a very large effective target mass M_T we obtain

$$\dot{U}_T = \dot{U}_T = 0 \tag{13}$$

so that the solution of Eqns (1)–(3) becomes trivial. There is no requirement for a resisting force of the backing (F_T). In solving the equations, depending on the input parameters the penetrator can be stopped before the ceramic is eroded, the penetrator can be completely eroded before it perforates the ceramic, or the ceramic itself can be eroded to zero thickness. In the latter case the residual projectile mass and velocity are obtained.

Using the residual projectile mass and velocity a plugging program [31] can be used to see if a thick backing is perforated by plugging by a flat ended fragment, or a program can be used to calculate the residual depth of penetration into a semi-infinite metal target [32]. An alternative simpler approach is to use the equation

$$1/2M_P\dot{U}_P^2 \leqslant \pi/2D_P^2 Y_T b \tag{14}$$

to relate the residual kinetic energy (LHS) to the work done in ductile hole formation (RHS). Here the symbols are as used before, except that b is the thickness of a finite backing in which case the inequality determines whether penetration occurs, or for a semi-

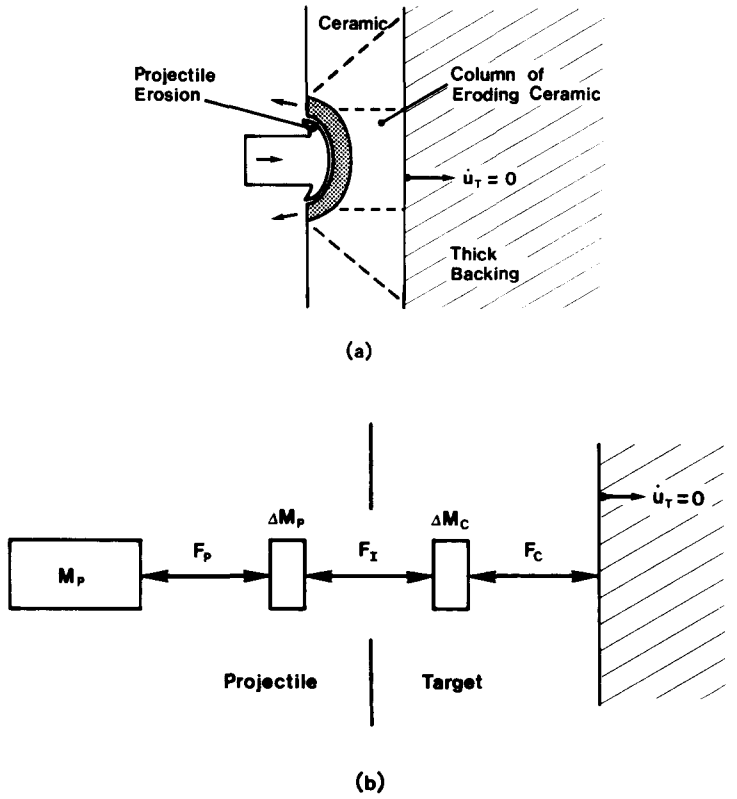

FIG. 3. Model concept for the thick backing problem where it is assumed that the backing remains effectively stationary whilst the ceramic is eroded. (a) Schematic and (b) lumped mass model.

infinite target b becomes the depth of penetration using the equality. Equation (14) uses the simpler Taylor model of ductile hole formation [29,30] and is equivalent to Eqn (12) for the thinner targets. This last approach is expected to be less accurate for the blunt fragments exiting from the ceramic, however it is presented as it is a useful simpler form. The most satisfying aspect of the models for thin and thick backings is that when the same strength Y_C is used for the ceramic, it is observed that the thin target and thick target approaches tie together well at the transition with increasing backing thickness. The most significant approximation, which prevents extension to very high velocities is the neglect of radial inertia which has not been included for the same reasons it has not been included in the thin backing model, i.e. a mathematically suitable treatment is not available.

3. SELECTION OF MATERIAL STRENGTH DATA

The penetrator undergoes large strain plastic flow on impact with the ceramic, thus a figure for ultimate tensile strength can be used in the modelling of its deformation. Because in many cases penetrators are hard, they are materials where there is little work hardening and within the accuracy of the model a figure for yield stress or the approximate equivalent, diamond pyramid hardness divided by 2.9 [33], should also be satisfactory. Work hardening is not included in the model so the response of the penetrator is determined entirely by its assumed ideal rigid/plastic resistance to plastic flow. Diamond pyramid hardness data is simple to obtain.

The metallic backing material has a failure strain dependent on its work hardening properties, and backing material stress strain data was therefore fitted to Eqn (8) for the thin target problem. For the thick backing or semi-infinite backing problems, curve fitting of the backing material and projectile data to appropriate forms for thick target penetration models was also required [31,32].

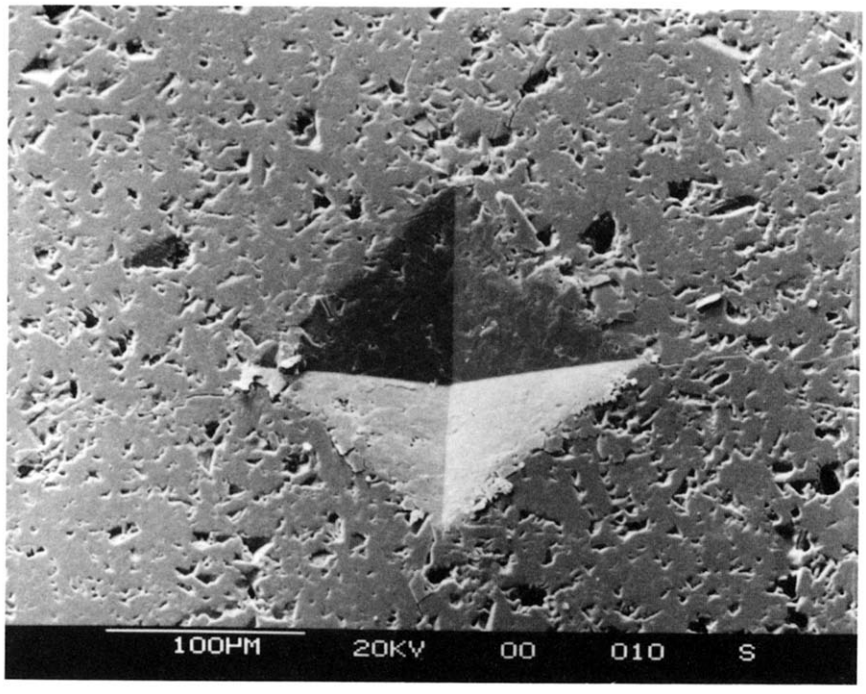

FIG. 4. Typical Vickers diamond pyramid indentation into a ceramic.

The major decision involves the selection of a suitable strength level for the ceramic representing its resistance to the penetrator or resistance to ceramic being displaced or eroded. The rate of erosion will be determined by yielding and cracking beneath the penetrator. Quasi-statically a blunt indenter forced into a ceramic causes yielding and fracture and the pressure beneath the indenter is a measure of hardness of the ceramic. Figure 4 shows a typical Vickers indentation in an alumina tile where cracking is evident from the corners of the indenter. If ceramics are assumed to obey the same laws of plastic flow as metals then the uniaxial flow stress can be obtained approximately from the hardness by dividing by 2.9 [33]. Initial computations using some data presented by Mayseless *et al.* [4] (Fig. 5) show an underestimate of the 12.7 mm projectile data (referred to as Berkeley data, henceforth), however the computations also showed the ceramic was not eroded under these conditions so there was no test of the appropriate flow stress properties of the ceramic. The comparison with the 7.62 mm projectile data of Wilkins (referred to as Livermore data) given in the same work indicates an underestimate if hardness divided by 2.9 is used as the ceramic flow stress and an overestimate by about the same amount if hardness is used, Fig. 5(a). The separation into two distinct slopes of the plots of theoretical curves for Wilkins experiments in Fig. 5(a), particularly noticeable for the lower strength level computations, is due to the onset of erosion at the higher backing thickness, where the impact velocity to cause perforation is necessarily higher, with the consequent shrinking of the loaded zone as depicted in Fig. 2(c). On the basis of this data it appears that hardness divided by some factor between 1.0 and 2.9 is an appropriate strength parameter for the ceramic. This would mean that cracking and ejection of material is easy and reduces the build-up of hydrostatic constraint in the dynamic problem.

Comparison with the full range of data provided by Wilkins [1] for four ceramic thicknesses did not, however, fit this picture easily. To fit Wilkins data it was necessary to increase the ceramic effective strength with thickness such that for thick plates the appropriate strength is close to the hardness. The fit to Wilkins [1] data using hardness as the effective ceramic strength is shown in Fig. 6. It is best described as a reasonable fit to the data. Rather than curve fit exactly to empirical data by playing with strength parameters, it was decided to use hardness throughout as the strength measure and

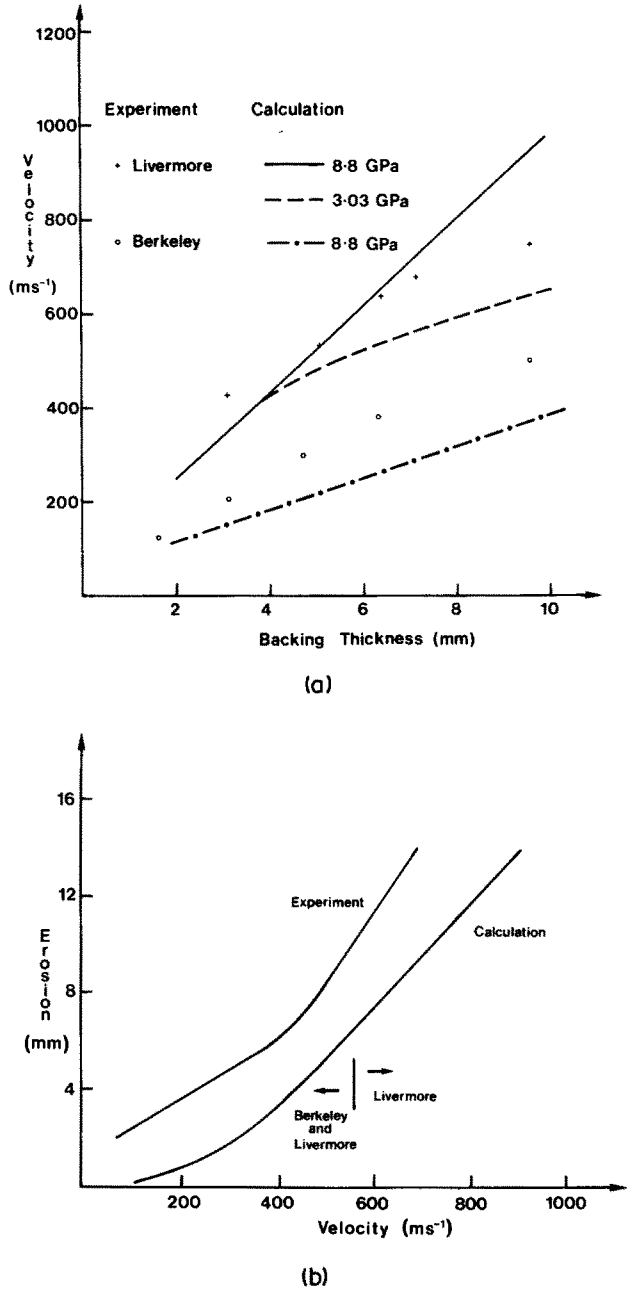

FIG. 5. (a) Comparison of ballistic limit predictions using the model for thin backings with data presented by Mayseless *et al.* [4]. For the Livermore data, due to Wilkins [3], two values of ceramic strength have been used; 8.8 GPa corresponding to the hardness and 3.03 GPa corresponding to hardness divided by 2.9. (b) Comparison of penetrator erosion calculated using the present model with the experimental curve of Mayseless *et al.* [4].

concentrate on the reliability of the computational approach and what it illustrates in the physics of perforation of ceramic composite armours.

Several other measures of strength are possible. The most obvious is the Hugoniot elastic limit, however this was not used as it is difficult and expensive to generate the data, values are tabulated for only some ceramics of interest and in any case the values are similar to the strength levels in hardness tests. Other possible measures are the ceramic compressive strength, or some combinations of strength measures [5,6]. The appropriate strength parameters to use for ceramics subject to ballistic impacts have been examined by Sternberg

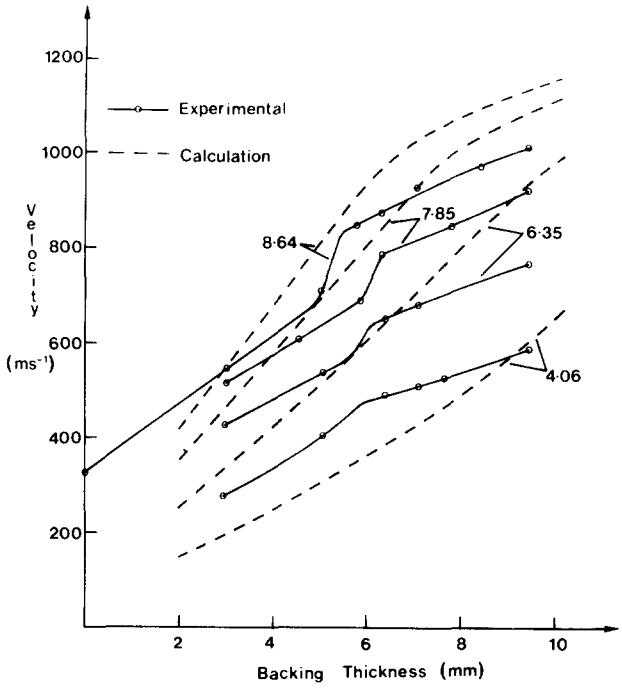

FIG. 6. Comparison of ballistic limit computations with experimental data of Wilkins [3] for four thicknesses of AD85 alumina ceramic and over a range of backing thicknesses.

[34] who indicated that initially resistance to penetration may be governed by the indentation hardness but drop to some lower value as cracking precedes penetration, so that some lower value, a fraction of the indentation hardness, may be the appropriate average resistance. Sternberg [34] demonstrates that this strength parameter may increase as ceramic toughness increases, and it may depend on confinement.

4. COMPARISON WITH EMPIRICAL DATA

The value of the model in terms of analysing and describing the mechanisms involved in perforation of ceramic composite targets is best appreciated by comparing computations with existing experimental data. Such a process also allows the limitations of inbuilt assumptions to be tested. Comparison is made with data of several types from several sources. In all cases ceramic strength and material stress/strain data were gleaned from the best sources available, however, in general, whilst it may be for the same material type and condition as used in the experiments, it should best be described as typical.

The fit of computations to the results of Mayseless *et al.* [4] in Fig. 5(a) could be considered reasonable. For the calculations on the Berkeley experiments there was no erosion of the ceramic and variations in ceramic strength will not improve the agreement. For all these computations the projectile erosion was part of the output and this is compared with the experimental curve of Mayseless *et al.* [4] for projectile erosion in Fig. 5(b). The form is correct, however, there is an underestimate of about 2 or 3 mm in the amount of erosion. As the model is for a flat ended penetrator, and the experimental work involved penetrators with a pointed nose several millimetres in length which would be readily broken, the difference between the experiment and the model is easily understood. In fact at very low velocities the experimental data shows a step jump in the magnitude of erosion.

The influence of ceramic erosion on predictions is illustrated in the computations of Fig. 6. The reason for the two distinct slopes in the calculated curves is the reduction in the effective loaded volume of ceramic, due to erosion, and backing as represented in Fig. 2(c); without this change in volume the graphs would continue at the initial slope. It is noted that for each ceramic thickness the slope change in the calculated curves occurs

consistently over a narrow velocity range which is determined by the ceramic strength. In contrast to this, Wilkins' experimental data shows a discontinuity consistently occurring at approximately the same backing thickness for each of the ceramic thicknesses. The most plausible explanation of this difference is that a lower stiffness in thinner ceramic tiles allows easier bending to a strain at which fracture is initiated, reducing the effective strength of thinner tiles. The overall agreement between the calculations and the experiment is seen to be good when the pairs of experimental and calculated curves are examined individually. As indicated above, one can improve the fit by selecting appropriate ceramic strength figures which increase with tile thickness, however this then becomes a curve fitting exercise with less meaning in the results. Certainly a valid approach would be to use ballistic testing and the model together under conditions where ceramic erosion is expected, in order to gauge the effective ceramic strength for those impact conditions. Rosenberg and Yeshurun [6] pointed out that, contrary to their expectations, some of Wilkins' data show no correlation between ballistic efficiency and compressive strength. From the present model this is in fact seen to be quite reasonable as Wilkins' data generally refers to conditions with backings which are thin enough that ceramic erosion, and hence strength, is of no significance. Under such conditions the effects of the ceramic are to induce erosion of the softer penetrator, and in the mass of ceramic cone material which must be accelerated ahead of the penetrator. The experiments of Rosenberg and Yeshurun [6] are on semi-infinite backings. As seen in Fig. 6, even for the relatively low strength AD-85 alumina, it is with the thicker backing where erosion of the ceramic occurs that the ceramic strength limits the rate of increase in performance with backing thickness. Observations by Wilkins [1,3] of projectile erosion with little perforation for the first 15–20 μs after impact may be considered to correlate with the acceleration phase in the present model, or for targets where erosion occurs it may also relate to a high initial resistance to ceramic erosion until such time as significant cracking and fragmentation has occurred, as discussed by Sternberg [34].

The effect of ceramic and backing thicknesses are again shown in Fig. 7 for the data of Wilkins *et al.* [2] using aluminium backed boron carbide tiles. The calculations give the correct ordering with ceramic and backing thickness and are as close to the experimental data as could be expected given the approximations in the model. In this case the model

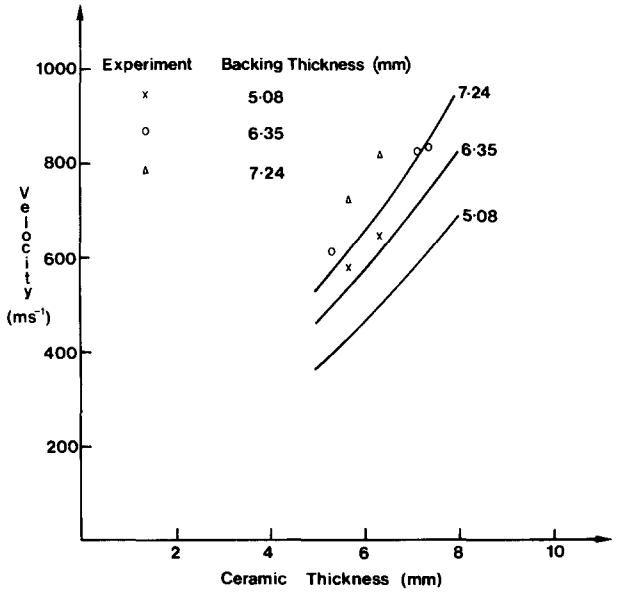

FIG. 7. The comparison of model computations with experimental data of Wilkins *et al.* [2] for aluminium backed boron carbide tiles. Curves represent model computations for the three backing thicknesses indicated.

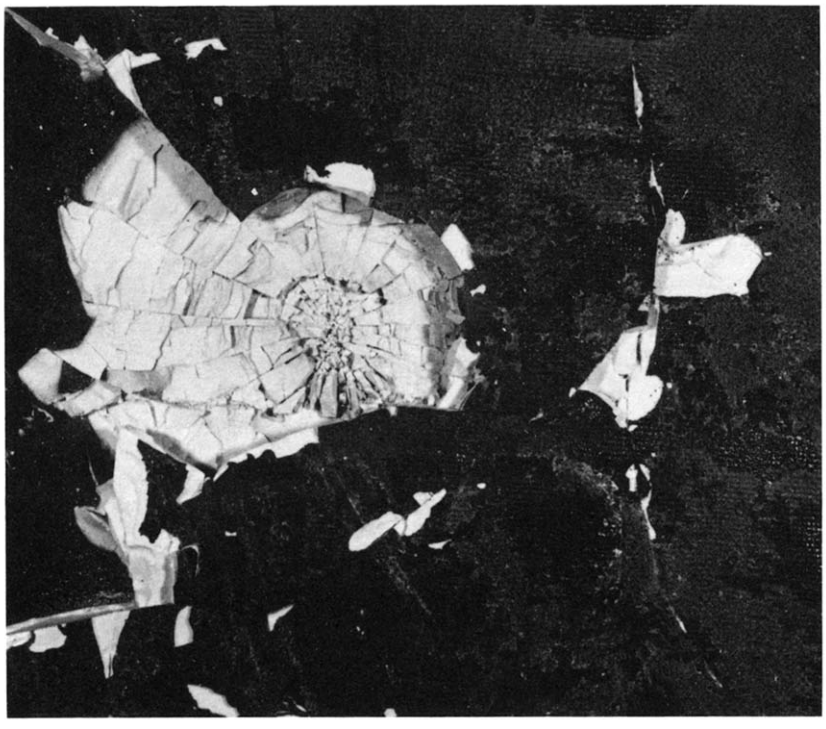

FIG. 8. An aluminium backed AD85 alumina target after impact by a steel cored armour piercing projectile below the ballistic limit, showing the radial and circumferential cracking and the maintenance of ceramic material between the projectile and the backing.

predicts no ceramic yielding, and hence no erosion, of the tiles. This is not meant to imply that the ceramic does not fragment, just that in the time frame of the ballistic event it is not eroded from its position ahead of the projectile. That ceramic fragmentation and erosion are not necessarily the same is shown by Fig. 8 which shows debris from the impact of an armour piercing round on an AD85 alumina target. Despite significant fragmentation the result of inertia and a resilient adhesive bond is to keep a large part of the fracture conoid in place.

Results for three different ceramics are shown in Fig. 9. The empirical data of Wilkins *et al.* [2] ranks the ceramics in terms of performance and the order of the ranking given by the model calculations is the same. The model estimates of ballistic limit are reasonably good. The areal density scale used in Fig. 9 compares ballistic limits at the same tile weight per unit area for three ceramics of different density. If instead a thickness axis was used, so that ballistic limits are compared at the same tile thickness, then both the experimental data and the computations bunch together with no clear distinction. According to the model the slight difference between ceramics when compared on the basis of thickness is due only to density which determines the mass of material bounded by the cone crack which must be accelerated, unless ceramic erosion is observed, and for the thin backings under the present conditions erosion only occurred at the highest impact velocities for the AD85 alumina, as evidenced by a change in slope in Fig. 9.

The formulation of the present model uses stress/strain behaviour suitable for a metallic backing, hence some composite materials are presently excluded from consideration. However, Mayseless *et al.* [4] show data for a range of backing materials including several metals allowing the effect of backing material to be examined for some cases as in Fig. 10. This comparison shows the calculated magnitude and ordering of performance using the model to be correct, however for these results the model consistently underestimates the ballistic limits.

Wilkins [1] also presented a comparison of the performance of sharp and blunt penetrators against AD85 alumina. The present model is for blunt penetrators and its

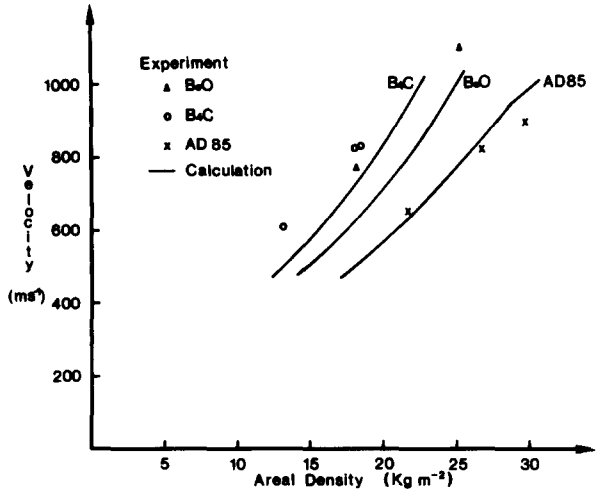

FIG. 9. Model computations compared to Wilkins *et al.* [2] empirical data for three different ceramic materials, beryllium oxide, AD85 alumina and boron carbide.

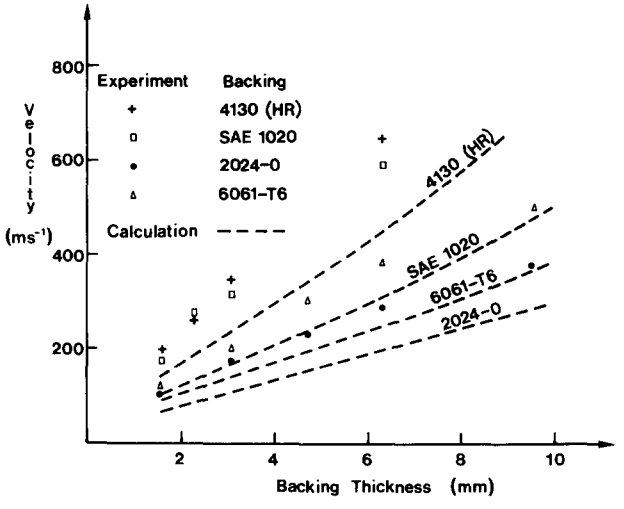

FIG. 10. The effect of backing material, comparing Mayseless *et al.* [4] empirical data for two steels, 4130 (HR) and 1020, and two aluminiums, 6061-T6 and 2024-O, with model calculations.

ballistic limit predictions are compared with Wilkins' [1] data in Fig. 11. Unfortunately the computations fit the sharp penetrator data better. The comparison, whilst emphasising the effect of nose shape, highlights the approximate nature of the present approach.

The model treatment for the situation of a thick backing can be compared with the data of Bless *et al.* [35] who backed alumina tiles with semi-infinite aluminium blocks. The experimental data comprise the depth of penetration into a semi-infinite block x compared with the depth when the block is covered with a ceramic tile R as presented in Table 1, where the ceramic tile thickness is C. Computations of penetration into the semi-infinite block were made with a deep penetration model [32] using the initial impact conditions to calculate x. For the case with the ceramic tile the model for a tile on a thick backing, Fig. 3, was used to treat the ceramic penetration and the output from these calculations used as input for the same deep penetration model to calculate R. In a small number of cases in which a sharp, hard penetrator was involved, a ductile hole formation model was more appropriately used for the calculation into a semi-infinite aluminium block. In the majority of cases Table 1 shows reasonable agreement. In most of those where agreement is poor, the impact velocity was far in excess of that where any of the models are expected

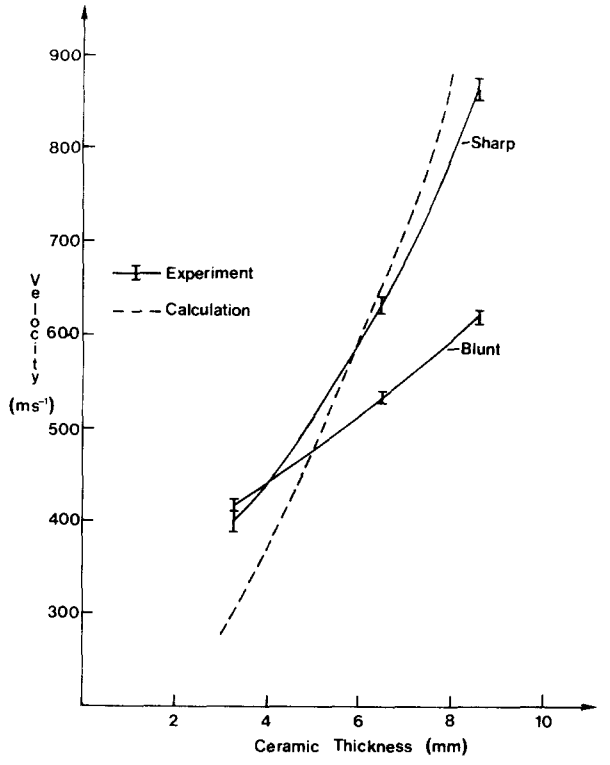

FIG. 11. Effect of projectile shape. The experimental data of Wilkins [1] is for sharp and for blunt penetrators, whilst the model computations assume a blunt penetrator.

TABLE 1. COMPARISON OF CALCULATED PENETRATION DEPTHS INTO ALUMINIUM COMPARED TO EXPERIMENTS OF BLESS *et al.* [35]*

S.N.†	U_0 (km s^{-1})	C (mm)	Projectile	X (mm) Exp.	X (mm) Calculation	R (mm) Exp.	R (mm) Calculation
4-324	2.55‡	9.3	8 g Ta rod	93	77	96	65
4-325	1.96‡	9.3	8 g Ta rod	74	56	84	46
6-777	1.35	9.3	8 g Ta rod	48	36	36	33
6-778	0.61	6.3	8 g Ta rod	11	9	4.8	0
6-967	0.70	9.19	8 g Ta rod, Sharp	16	12.7	5.3	0
6-958	1.66	12.7	12.7 FSP	33	27	14.8	18
6-969	1.01	9.14	12.7 FSP	17.5	14	4.8	0
4-452	2.30‡	9.14	7.62 APM2	91	45 (429)	64	41
9-843	0.84	9.14	7.62 APM2	48	10.8 (57)	1	0
10-452	0.78	6.35	7.62 APM2	48	8.6 (49)	1	0
9-1117	0.94	9.14	7.62 AMP2	51	11.9 (72)	1	0
6-832	0.88	9.14	7.62 W2 APM2	115	19 (126)	4	11.5
6-966	1.64	9.14	7.62 APM2	73	29 (218)	30	24
4-579	2.70‡	9.14	6061-T6 APM2	51.5	57.5	31.3	56
4-596	2.80‡	9.14	7075-T6 APM2	53	61	39.4	60
6-1122	1.47	9.14	7075-T6 APM2	31	17	3	0

*Calculations of penetration depth were generally performed with a deep penetration model [26,27] except for cases indicated by ( ) because a hard sharp penetrator is concerned and in these cases the model of Taylor for ductile hole formation was used, i.e. Eqn (14). Those results which are underlined are considered effective calculations. Some reasons for poor agreement in other cases are discussed in the text. Shots No. 4-324 and 4-325 involved the use of a cover plate over the ceramic, and this was accounted for approximately in the computations.

†S.N. = Shot No., U_0 = impact velocity, C = ceramic thickness, X = depth into aluminium with no ceramic cover, R = depth into aluminium with ceramic tile, FSP = fragment simulating projectile.

‡Shots thus indicated were at impact velocities far above that at which any of the models are expected to be valid.

to work (i.e. $>1.5\,\mathrm{km\,s^{-1}}$). In a couple of cases where computational agreement was obtained, where the impact velocity was beyond the range of the models, it is considered a coincidence in the present instance, and these cases are not highlighted in Table 1 as effective computations. At least in one case (Shot 4-452), Bless *et al.* [35] indicate that their "experimental" depth of penetration is only "estimated".

In making the above calculations with the method for the thick backing problem it was noted that ceramic erosion occurred whilst the penetrator was above some critical velocity depending on the ceramic strength. Below this velocity only the penetrator was eroded and decelerated, with the calculations stopping when the penetrator was reduced to zero mass or velocity. In those cases where the impact velocity was just above the value for erosion of the ceramic, the deceleration during the interaction was sufficient to reduce the projectile velocity below the critical value and ceramic erosion stopped before the ceramic in front of the projectile was completely removed. In all cases where the ceramic was not perforated Table 1 shows zero residual perforation. In practice a few millimetres of deformation is always observed due to fracture of the ceramic and impact of the residual debris.

Using the same test configuration Rosenberg and Yeshurun [5,6] plot data as density times depth for the semi-infinite aluminium backing versus density times thickness for the ceramic tile. Figure 12 shows the data of Rosenberg and Yeshurun [5,6] for impact of a 12.7 mm projectile at $920\,\mathrm{ms^{-1}}$ on AD85 alumina compared with a calculated line using their figure for ceramic effective strength of 4.2 GPa. To make the model calculation and experiment coincident requires the strength be reduced to 4.05 GPa. Their experimental

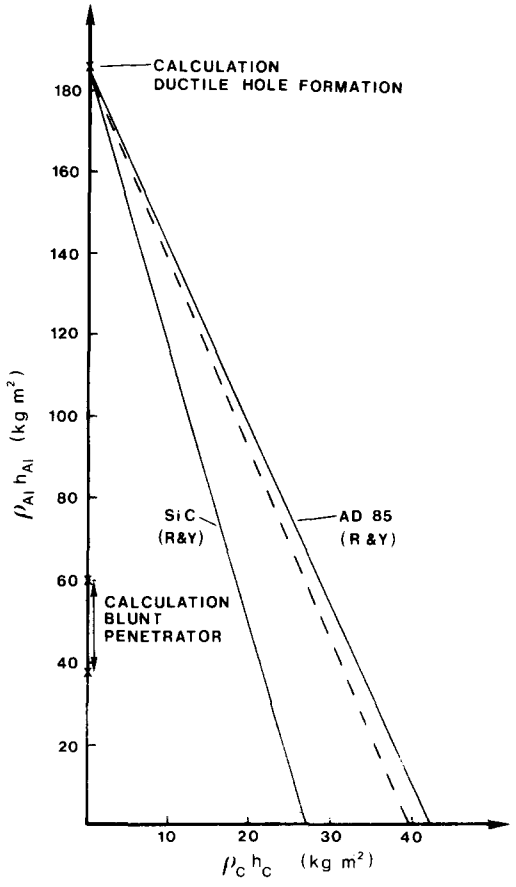

FIG. 12. Data of Rosenberg and Yeshurun [5,6], continuous lines, plotted as density times depth for the aluminium backing against density times thickness for the ceramic tile, for AD85 alumina and silicon carbide. A calculated line, dashed, is also shown for the AD85 alumina, and calculated depths into bare aluminium for pointed and blunt penetrators are shown.

line for silicon carbide is also shown and to achieve coincidence a strength of 4.85 GPa was required in the model, whereas Rosenberg and Yeshurun [5,6] indicate an effective strength under ballistic conditions of 7.7 GPa. A strength of 7.7 GPa and an impact velocity of 920 ms^{-1} only allowed limited erosion of the ceramic tile using the present method. The model for ductile hole formation [29,30] was used to calculate the effective depth of penetration when no ceramic tile was used and the agreement was excellent. Also shown in Fig. 12 is the range of penetration depths expected for a blunt penetrator, the higher value assuming no penetrator deformation and the lower value allowing projectile deformation. This plot highlights a number of interesting aspects. Whilst use of an aluminium backing provides extra sensitivity in testing the ceramic this is achieved because the pointed penetrator has a much greater penetration capability than has an equivalent blunt penetrator into the aluminium. Use of the ceramic results in a large reduction in depth of penetration caused by blunting of the penetrator as well as by the effects due to erosion and velocity reduction. It must therefore be kept in mind that this simple graphical comparison is sampling the effects of more than one physical process. The strength data used to obtain agreement is close to that suggested by Rosenberg and Yeshurun [5,6] but a fraction of the hardness of these ceramics. This accords with the discussion of Sternberg [34], and suggests this method as a rapid experimental procedure for defining the ceramic strength to be used in ballistic calculations. The appropriate strength value may also be a function of velocity, being low at low velocities where cracking can precede penetration, but higher as velocity increases closer to the rate of propagation of the damage front [17]. Effective ceramic strength may also depend on the type of ballistic test and on the model used for analysis of the data, whilst these models remain approximate.

5. DISCUSSION

There is no pretence that the models presented in the present work are to be considered an exact simulation of the physics of impact, however the straightforward descriptions which they embody lead to reliable and relatively simple algorithms which give reasonable quantitative estimates of ceramic performance. In addition the predictions of changes with variations in ceramic and backing material type and thickness, and projectile material and dimensions are such that the models should be useful for parametric studies and for guiding experiments and design. The concepts as presented in Figs 1–3 therefore probably embody most of the principal features of the impact event. More accurate physical modelling with increased complexity of the algorithms can be expected to lead to better predictions of performance. Approximations on aspects of both the physics and the material properties are so gross that the degree of concurrence with experiment over such a wide range could be considered truly remarkable.

A major omission is the neglect of radial inertia. Not only is the momentum of eroded projectile material destroyed, but also it must be ejected laterally at some velocity. The treatment used by Johnson [26] for high rate compression was not easily adopted in the present instance as the radial inertia force becomes excessive as the thickness of the deforming zone becomes small which, with the present model, is dependent on the time step. The most profitable approach would appear to be to consider the eroded projectile material as having a momentum change associated with a velocity change from $\dot{U}_P$ to some radial ejection velocity $\dot{U}_R$, rather than by having its momentum destroyed as in the conventional modified Bernoulli approach [25]. At present the extra variable would seem to make the equations insoluble. This would however maintain the same logic as considering an increase in momentum associated with the velocity $\dot{U}_C$ picked up by the eroded ceramic, and it may be possible to relate $\dot{U}_C$ and $\dot{U}_R$ in some way.

In treating the backing deformation which is largely a dishing or bulge formation problem, the location of the hinge is a convenient conjecture. There is no doubt that in practice both significant elastic contributions to deflection and expansion of the hinge radially influence both the energy absorption and the effective observed ductility of the

backing material. The simple linear thickness variation and the choice of instability criterion fortunately give overall deflections which are in accord with experience.

The deflection of the backing increases the radial and circumferential cracking in the ceramic. When bending occurs the resultant lack of support due to the bending allows ejection of fragmented ceramic from the back, and in addition ejection of ceramic on the impact side is resisted less than the extrusion of material when the penetrator gets deeper into the ceramic tile. For this problem there is almost a complete lack of knowledge on material continuity and consolidation at any time. The whole question of how ceramic fragmentation influences effective strength is unresolved. The use of hardness in the present instance as a guide to strength is seen to be an effective starting point.

Projectile shape is limited to the assumption of a flat ended cylinder. This is seen to highlight how approximate the model is in Fig. 11 as the model does not have the sensitivity to at least plot nearer to experimental data for the blunt projectiles. Generally ceramics negate, by fracture, the influence of a sharp nose as is highlighted by the discussion of Fig. 5(b) and as shown in the data of Wilkins [1] in Fig. 11, easier fracture of pointed projectile makes them less effective penetrators, higher ballistic limit. Questions on projectile shape will not be resolved by one dimensional models such as these and must rely on experiment and two and three dimensional simulations for detailed examination.

Despite the above difficulties, and the questions of ceramic effective strength in particular, the comparisons in this study show that by focusing on material inertia and acceleration aspects, and by using approximate strength of materials considerations to treat material distortion and failure, that models can be developed which are effective tools for the study of ceramic armour behaviour. The method should not be used for the prediction of performance, rather as a guide in understanding the interactions. Thus the model for thick backings may, by simulating experiments, enable studies of the effective pressure at which erosion occurs and how this is influenced by material and confinement.

6. CONCLUSIONS

This work has presented two models for the perforation of ceramic composite armours, one for the perforation of targets with thin backing plates, which deform by bending away under the influence of the ceramic fracture conoid to fail by a biaxial tensile fracture, and the other for targets with a thick backing, where the backing remains undeformed whilst the ceramic erodes and is then perforated by the residual projectile fragment. The details of ceramic fragmentation are avoided in the model which treats the dynamics of movement of blocks of material with macroscopic failure criteria for both ceramic and backing. Comparisons of computations with empirical data demonstrate a good correlation, and the models can be used for parametric studies, to assist with the analysis of experimental data and for design. Ceramic hardness is used as a strength parameter, however the consideration of ceramic strength appropriate to ballistic impact is considered a major aspect for further investigations.

REFERENCES

1. M. L. Wilkins, Mechanics of penetration and perforation. *Int. J. Engng Sci.* **16**, 793–807 (1978).
2. M. L. Wilkins, C. F. Cline and C. A. Honodel, Fourth progress report of light armour program (Report UCRL-50694). Livermore: Lawrence Radiation Laboratory, University of California (1969).
3. M. L. Wilkins, Computer simulation of penetration phenomenon, in *Ballistic Materials and Penetration Mechanics* (edited by R. C. Laible), pp. 225–252. Elsevier (1980).
4. M. Mayseless, W. Goldsmith, S. P. Virostek and S. A. Finnegan, Impact on ceramic targets. *J. Appl. Mech.* **54**, 373–378 (1987).
5. Z. Rosenberg and Y. Yeshurun, An empirical relation between the ballistic efficiency of ceramic tiles and their effective compressive strength. *Proc. 10th Int. Symp. on Ballistics*, ADPA, San Diego, California (1987).
6. Z. Rosenberg and Y. Yeshurun, The relation between ballistic efficiency and compressive strength of ceramic tiles. *Int. J. Impact Engng* **7**, 357–362 (1988).

7. I. MELLGARD, L. HOLMBERG and L. G. OLSSON, An experimental method to compare the ballistic efficiencies of different ceramics against long rod projectiles. *Proc. 10th Int. Symp. on Ballistics*. ADPA, San Diego, California (1987).
8. B. NICOL, S. D. PATTIE, R. G. O'DONNELL and R. L. WOODWARD, Fracture of ceramics in composite armours, in fracture mechanics in Engineering Practice, Conference of Australian Fracture Group, Melbourne University (1988).
9. R. L. WOODWARD, R. G. O'DONNELL, B. J. BAXTER, B. NICOL and S. D. PATTIE, Energy absorption in the failure of ceramic composite armours. Materials Forum (1989).
10. W. PAVEL, H.-J. RAATSCHEN, R. SCHWARZ, H. SENF and H. ROTHENHAUSLER, Experimental and numerical investigations of the failure behavior of glass targets under impact loading by rigid projectiles. *Proc. 10th Int. Symp. on Ballistics*, ADPA, San Diego, California (1987).
11. F. C. FRANK and B. R. LAWN, On the theory of Hertzian fracture. *Proc. R. Soc.* **A229,** 291–306 (1967).
12. C. G. KNIGHT, M. V. SWAIN and M. M. CHAUDHRI, Impact of small steel spheres on glass surfaces. *J. Mat. Sci.* **12,** 1573–1585 (1977).
13. B. R. LAWN and M. V. SWAIN, Microfracture beneath point indentations in brittle solids. *J. Mat. Sci.* **10**, 113–122 (1975).
14. B. LAWN and R. WILSHAW, Review indentation fracture: principles and applications. *J. Mat. Sci.* **10**, 1049–1081 (1975).
15. P. OSTOJIC and R. MCPHERSON, A review of indentation fracture theory: its development, principles and limtations. *Int. J. Fract.* **33**, 297–312 (1987).
16. R. L. WOODWARD, Some aspects of cone crack propagation in finite thickness glass plates. In The Material Wealth of the Nation, Proceedings of Institute of Metals and Materials Australasia Bicentennial Conference, Sydney, Australia, **1,** 111–118 (1988).
17. U. HORNEMANN, H. ROTHENHAUSLER, H. SENF, J. F. KALTHOFF and S. WINKLER, Experimental investigation of wave and fracture propagation in glass slabs loaded by steel cylinders at high impact velocities, in *Mechanical Properties at High Rates of Strain* (edited by J. HARDING), pp. 291–298, Institute of Physics Conference Series No. 70, Institute of Physics. Bristol and London (1984).
18. L. H. L. LOURO and M. A. MEYERS, Effect of stress state and microstructural parameters on impact damage of alumina-based ceramics. *J. Mat. Sci.* **24,** 2516–2532 (1989).
19. F. LONGY and J. CAGNOUX, Plasticity and microcracking in shock-loaded alumina. *J. Am. Ceramic Soc.* **72,** 971-979 (1989).
20. Y. YESHURUN, D. G. BRANDON, A. VENKERT and Z. ROSENBERG, The dynamic properties of two-phase alumina/glass ceramics. *J. Phys. Coll.* **C3, 49,** C11–C18 (1988).
21. R. G. O'DONNELL, to be published.
22. C. TRACY, M. SLAVIN and D. VIECHNICKI, Ceramic fracture during ballistic impact, in *Advances in Ceramics, Fractography of Glasses and Ceramics*, American Ceramic Society, **22,** 295–306 (1988).
23. R. ARROWOOD and J. LANKFORD Jr, Dynamic characterization of an alumina ceramic, South West Research Institute SWRI-6724, November (1982).
24. W. GOOCH Jr, US Army Ballistics Research Laboratory, private communication (1989).
25. A. TATE, A theory for the deceleration of long rods after impact. *J. Mech. Phys. Solids* **15,** 387–399 (1967).
26. W. JOHNSON, *Impact Strength of Materials*, p. 152. Arnold, London (1972).
27. W. JOHNSON, *Impact Strength of Materials*, p. 194. Arnold, London (1972).
28. W. JOHNSON and P. B. MELLOR, *Plasticity for Mechanical Engineers*, p. 187. Van Nostrand (1962).
29. G. I. TAYLOR, The formation and enlargement of a circular hole in a thin plastic sheet. *J. Mech. Appl. Math.* **1,** 103–124 (1948).
30. R. L. WOODWARD, The penetration of metal targets by conical projectiles. *Int. J. Mech. Sci.* **20**, 349–459 (1978).
31. R. L. WOODWARD and M. E. DE MORTON, Penetration of targets by flat-ended projectiles. *Int. J. Mech. Sci.* **18**, 119–127 (1976).
32. R. L. WOODWARD, Penetration of semi-infinite metal targets by deforming projectiles. *Int. J. Mech. Sci.* **24**, 73–87 (1982).
33. D. TABOR, *The Hardness of Metals*. Clarendon Press, Oxford (1951).
34. J. STERNBERG, Material properties determining the resistance of ceramics to high velocity penetration. *J. Appl. Phys.* **65,** 3417–3424 (1989).
35. S. J. BLESS, Z. ROSENBERG and B. YOON, Hypervelocity penetration of ceramics. *Int. J. Impact Engng* **5**, 165–171 (1987).